Evidence of nontermination of collective rotation near the maximum angular momentum in ^{75}Rb

P. J. Davies,[1,*] A. V. Afanasjev,[2,3] R. Wadsworth,[1] C. Andreoiu,[4] R. A. E. Austin,[5,†] M. P. Carpenter,[6] D. Dashdorj,[7] P. Finlay,[4]
S. J. Freeman,[6,8] P. E. Garrett,[4] A Görgen,[9] J. Greene,[6] G. F. Grinyer,[4] B. Hyland,[4] D. G. Jenkins,[1] F. L. Johnston-Theasby,[1]
P. Joshi,[1] A. O. Macchiavelli,[10] F. Moore,[6] G. Mukherjee,[6,‡] A. A. Phillips,[4] W. Reviol,[11] D. Sarantites,[11] M. A. Schumaker,[4]
D. Seweryniak,[6] M. B. Smith,[12] C. E. Svensson,[4] J. J. Valiente-Dobon,[4,§] and D. Ward[10]

[1]*Department of Physics, University of York, Heslington, York YO10 5DD, United Kingdom*
[2]*Department of Physics and Astronomy, Mississippi State University, Mississippi 39762, USA*
[3]*Laboratory of Radiation Physics, Institute of Solid State Physics, University of Latvia, LV-2169 Salaspils, Miera strasse 31, Latvia*
[4]*Department of Physics, University of Guelph, Guelph, Ontario N1G 2W1, Canada*
[5]*Department Physics and Astronomy, McMaster University, Hamilton, Ontario L8S 4K1, Canada*
[6]*Physics Division, Argonne National Laboratory, 9700 South Cass Avenue, Argonne, Illinois 60439, USA*
[7]*North Carolina State University, Rayleigh, North Carolina 27695, USA*
[8]*Department of Physics and Astronomy, University of Manchester, Manchester, M15 9PL, United Kingdom*
[9]*CEA Saclay, IRFU, Service de Physique Nucléaire,F-91191 Gif-sur-Yvette, France*
[10]*Lawrence Berkeley National Laboratory, Berkeley, California 94720, USA*
[11]*Department of Chemistry, Washington University, St. Louis Missouri 63130, USA*
[12]*TRIUMF, 4004 Wesbrook Mall, Vancouver, British Columbia, V6T 2A3, Canada*

Two of the four known rotational bands in ^{75}Rb were studied via the ^{40}Ca(^{40}Ca,αp)^{75}Rb reaction at a beam energy of 165 MeV. Transitions were observed up to the maximum spin I_{max} of the assigned configuration in one case and one-transition short of I_{max} in the other. Lifetimes were determined using the residual Doppler shift attenuation method. The deduced transition quadrupole moments show a small decrease with increasing spin, but remain large at the highest spins. The results obtained are in good agreement with cranked Nilsson-Strutinsky calculations, which indicate that these rotational bands do not terminate, but remain collective at I_{max}.

The atomic nucleus is a unique testing ground for a number of physical phenomena, which either do not exist or cannot be verified experimentally, in other finite many-fermion quantum systems. One of these unique phenomena is a termination of rotational bands in a noncollective single-particle (terminating) state at I_{max}, where I_{max} is the maximum spin that can be built from a pure configuration. Although this phenomenon was studied in detail (see Ref. [1] for a review), it is only recently that earlier theoretical predictions [1–3], suggesting that not all rotational bands have to terminate in a noncollective state at I_{max}, have been confirmed by experiment [4,5]. In ^{74}Kr, two bands were observed up to I_{max} as was a third band one-transition short of I_{max} [4]. The deduced transition quadrupole moments showed a small decrease within a band with increasing spin, however, this decrease was not large enough to suggest a complete loss of collectivity at the maximum allowed spins. Cranked relativistic mean field (CRMF) [6] and cranked Nilsson-Strutinsky (CNS) [1] calculations reproduced the experimental data well and strongly indicated that the rotational structures do not terminate at I_{max}. These

calculations also suggested that the configurations of interest remain collective ($\varepsilon_2 \sim 0.2$, $\gamma \sim 20°$) at spins higher than I_{max}. In addition, a recent publication suggested that ^{73}Kr may not terminate at I_{max} [5]. In that work one rotational band was observed up to I_{max} and two other bands were observed to states close to I_{max}. As in the case of ^{74}Kr, CNS calculations for this nucleus suggest that these bands remain collective at and beyond the predicted terminating state. A comparison of the experimentally obtained dynamic moments of inertia to those predicted by the calculations suggests that the transition quadrupole moment of the bands in ^{73}Kr remains large in states close to the termination. However, the work performed for that article did not explicitly measure the transition quadrupole moments for these states or show that these bands extend beyond the expected terminating spins. These results suggested that nuclei bordering ^{74}Kr may be excellent candidates for further investigation of this novel phenomenon of nontermination of rotational bands. In the present work we provide clear evidence for this effect in the rotational structures in ^{75}Rb.

The phenomenon of nontermination of rotational bands was studied in the harmonic oscillator potential [1,2] and in a more realistic Nilsson potential [3]. Here we briefly outline its major features. In a harmonic oscillator potential, rotational bands do not terminate in a noncollective state at I_{max} if the deformation exceeds some critical value at low spin (see Fig. 2 in Ref. [1]). This is a consequence of the coupling of different N shells leading to the mixing of different configurations, which allows even higher spins than I_{max} to be

*pjd113@york.ac.uk
†Present address: Saint Mary's University, Halifax NS B3H 3C3, Canada.
‡Present address: Variable Energy Cyclotron Centre, Kolkata 700064, India.
§Present address: INFN, Laboratory Nationali di Legnaro, I-35020, Italy.

built within the mixed configuration. On the contrary, in a realistic potential, each single-particle orbital is described by its individual angular momentum j. Thus, it is possible to make a separation into high-j and low-j orbitals within the same N shell. As a consequence, known terminating bands are well classified in a scheme in which the configurations and their I_{max} are defined in terms of the distribution of particles and holes over low-j and high-j subshells [1]. However, similar to the harmonic oscillator potential, this scheme describing a pure configuration breaks down with increasing deformation. For example, in the $A \sim 75$ mass region, the mixing between low-j $p_{1/2}$, $p_{3/2}$, and $f_{5/2}$ and high-j $f_{7/2}$ orbitals in the $N = 3$ shell leads to mixed rotational bands that do not terminate at I_{max} [3,4]. The appreciable deformation of rotational bands in this region is the reason for strong mixing of the low-j and high-j orbitals.

While the borderline between terminating and nonterminating configurations is well defined in the case of the harmonic oscillator potential via the deformation of low-spin states (see Fig. 2 in Ref. [1]), no such clear distinction exists in the case of a realistic potential. The configurations with the same deformation at low spin can either terminate or not terminate at I_{max}; their behavior at I_{max} strongly depends on their internal structure. As a consequence, terminating and nonterminating configurations coexist in the same nucleus in the $A \sim 75$ mass region in model calculations. The determination of transition quadrupole moments up to or close to I_{max}, as well as the observation of the $I_{max} + 2$ state that belongs to the rotational band, are the best ways to distinguish nonterminating configurations from terminating ones.

In the present work we study ^{75}Rb, which contains one proton more than ^{74}Kr, hence one will expect configurations to terminate at similar values of I_{max} ($\sim 35\hbar$) to those seen in ^{74}Kr [4]. In this Rapid Communication we report on the behavior at high spin of transition quadrupole moments of two bands in ^{75}Rb. The modest decrease observed in the transition quadrupole moments with increasing spin, as well as model calculations, suggests that ^{75}Rb is only the second clear example of a nucleus where rotational bands do not terminate in a noncollective state at I_{max}.

Excited states in ^{75}Rb were populated via the ^{40}Ca (^{40}Ca, αp)^{75}Rb reaction. The 165 MeV beam of ^{40}Ca, provided by the Argonne Tandem Linac Accelerator System (ATLAS) at Argonne National Laboratory, was incident upon a 350 μg.cm^{-2} enriched ^{40}Ca target, which was flashed with 150 μg.cm^{-2} of Au on both sides to inhibit oxidation. All events where at least four γ rays were observed in prompt coincidence were recorded using the Gammasphere array [7], which contained 101 high-purity Compton suppressed germanium detectors. Charged particles from the reaction were detected using the Microball charged particle array [8].

The lifetime data reported in this Rapid Communication were obtained from the same data set as that reported in Ref. [9], where extensions to three of the four known bands [10] were discussed. In the present work the lifetimes of high-spin states in the $(\pi, \alpha) = (-, +1/2)$ and $(+, +1/2)$ configurations, where π is the parity of the band and α is its signature, were obtained. For convenience the $(\pi, \alpha) = (-, -1/2)$, $(-, +1/2)$, and $(+, +1/2)$ configurations will be referred
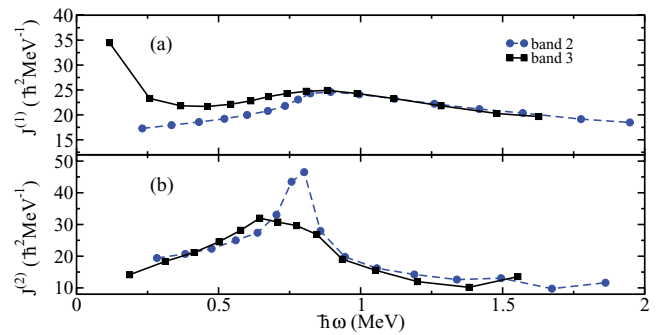
FIG. 1. (Color online) (a) Experimental kinematic and (b) dynamic moments of inertia as a function of rotational frequency.

to as bands 1, 2, and 3, respectively. These configurations are consistent with the assignments of the bands previously reported up to $\frac{47}{2}^-\hbar$, $\frac{73}{2}^-\hbar$, and $\frac{65}{2}^+\hbar$, see Fig. 5 in Ref. [9].

Furthermore, these configuration assignments are consistent with the ones at high spin referred to in the following discussion. Using the γ-ray energies of Ref. [9], the kinematic ($J^{(1)}$) and dynamic ($J^{(2)}$) moments of inertia were calculated, these are presented in Fig. 1. The frequency of the neutron $g_{9/2}$ paired band crossing is clearly evident at $\hbar\omega = 0.65$ MeV for band 3; the proton $g_{9/2}$ band crossing is blocked in this band. Simultaneous proton and neutron $g_{9/2}$ paired band crossings take place at $\hbar\omega = 0.80$ MeV in band 2. Above these frequencies no sudden change is observed in the values of $J^{(1)}$ or $J^{(2)}$ in either band.

To investigate the evolution of deformation as a function of spin we measured the lifetimes of the high-spin states in ^{75}Rb using the residual Doppler shift attenuation method (RDSAM) [11]. To achieve this, spectra were constructed so that they contained only γ rays emitted at a specified angle (θ). This angle is defined as that between the direction of the γ-ray emission and the beam axis from the target position. The spectra were produced by unpacking the data into triple events and sorting them into a noncompressed E_γ-E_γ-$E_{\gamma\theta}$ cube, where E_γ is the energy of a γ ray detected at any angle and $E_{\gamma\theta}$ is the energy of a γ ray detected at a specified angle θ. Gating conditions were set so that only data containing one α particle and one proton were included in the cube. To obtain spectra for the bands of interest in ^{75}Rb a projection of the cube was made onto the $E_{\gamma\theta}$ axis using γ-ray energy gates on the E_γ-E_γ axes. The γ-ray energy gates were carefully selected from the bands of interest in ^{75}Rb so that they introduced no contamination into the spectra and included the full width of the γ-ray transition. Additionally, to remove random coincident events, background spectra were created using the method of Starosta *et al.* [12] and subtracted from each of the γ-gated spectra. Figure 2 shows the representative spectra for γ rays emitted from band 2 at weighted angles of 53° and 127°, the residual Doppler shift is clearly evident in all the transitions shown. The angles given in Fig. 2 represent the weighted-average angle of the 35 forward-most and backward-most detectors in Gammasphere. Such a large grouping of detectors was required to measure the residual Doppler shift of the highest spin states (those above $I = \frac{57}{2}\hbar$), as these are the least well populated.
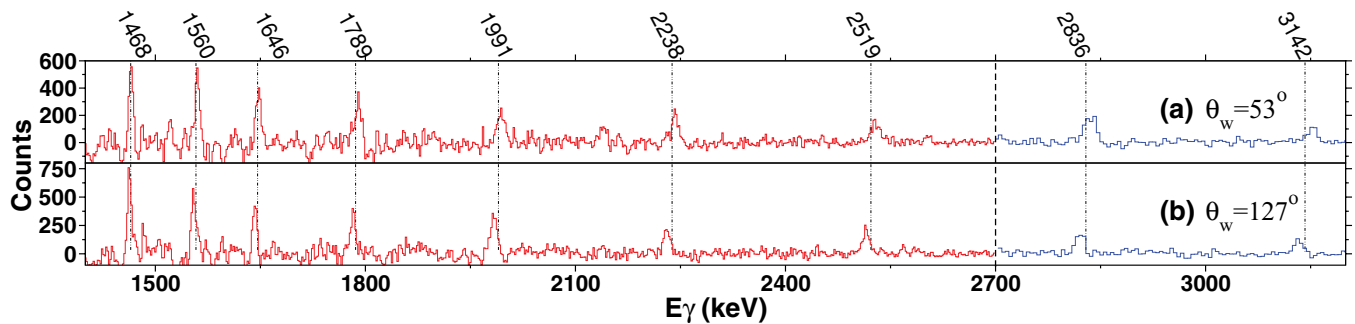
FIG. 2. (Color online) Panels (a) and (b) show partial γ-ray spectra for band 2 in ^{75}Rb that reveal the observed residual Doppler shifts. The energies of the γ rays are given at the top of the figure. The weighted angles θ_w, used to create these spectra, are shown in the two panels (see text for details). Note to clearly show the shift in the highest-energy transitions the binning changes from 2 keV per channel to 5 keV per channel at the thick dashed line.

For γ rays emitted below $\frac{57}{2}\hbar$ it was possible to make the same measurements using five groups of detectors at weighted angles 35°, 52°, 90°, 128°, and 145°. For γ rays emanating from the medium-spin states the measurements from both groupings of detectors were found to be consistent.

Figure 3 shows the measured fraction $F(\tau)$ of the Doppler shift plotted as a function of spin for bands 2 and 3 in ^{75}Rb, extracted using the RDSAM. It is clear, from the constant $F(\tau)$, that the levels where $I \lesssim 15$ are decaying once the recoiling nucleus has left the target and is traveling with a constant velocity. The opposite is true for levels where $I \gtrsim 15$, the increase in $F(\tau)$ is due to the slowing of the recoiling nucleus as it passes through the target. It should be noted that by definition $F(\tau) = 1$ is the maximum value the fractional Doppler shift can attain. However, this assumes the reaction takes place in the center of the target. Due to reactions taking place at other locations, larger values for $F(\tau)$ are permitted. The RDSAM analysis was carried out using the same techniques as those discussed in Refs. [4,13,14].

The experimental $F(\tau)$ values were fitted taking into account the slowing down process of the recoiling nuclei in the target and the Au backing. The slowing of the recoils was modeled using stopping powers obtained from the SRIM code [15]. The angular dependence of the α-particle detection efficiency for the Microball charged particle detector [16,17] was also taken into account. As the spectra, from which $F(\tau)$ were measured, are produced by γ-ray gates on low-spin
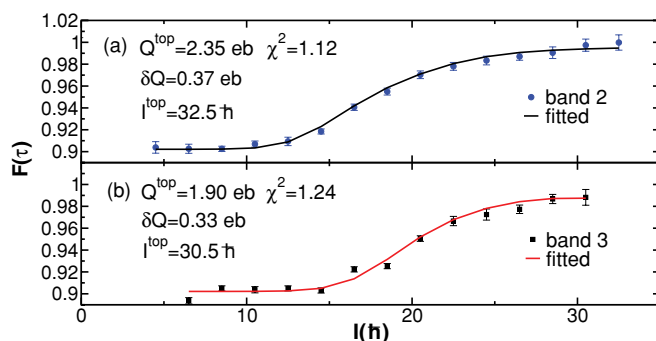
transitions, side feeding into these bands was also taken into account. In the present work, this was modeled using a series of four transitions with the same transition quadrupole moment as the state they are feeding. The decay of the nucleus was modeled using the empirical equation $Q_t(I) = Q_t^{\text{top}} + \delta Q_t \sqrt{I^{\text{top}} - I}$ [14] to fit the experimental data. Q_t^{top} is the transition quadrupole moment for the highest measured transition in the rotational band, δQ_t is the change in transition quadrupole moment within the band, I^{top} is the maximum measured spin within the band, and I is the spin of the state of interest. In the present work the values of I^{top} for bands 2 and 3 were $\frac{65}{2}\hbar$ and $\frac{61}{2}\hbar$, respectively. The fitted values of $F(\tau)$ along with the associated best-fit $Q_t^{\text{top}}(I)$ and δQ_t values are presented in Fig. 3, and the transition quadrupole moments extracted from the method are presented in Fig. 4(a). No double γ-ray energy gate combination could be found that would produce uncontaminated spectra with sufficient statistics for a RDSAM analysis of band 1.

A theoretical analysis was performed within the framework of the CNS [1] and CRMF [6] approaches. Since we are interested in high-spin behavior, pairing was neglected in both calculations. The validity of such an approximation is supported by the fact that $J^{(1)} \geqslant J^{(2)}$ at $\hbar\omega \geqslant 0.8$ MeV; this is a typical feature of rotational bands in an unpaired regime [1]. These two approaches have previously been successfully applied to the description of experimental data at high spin in neighboring nuclei such as ^{70}Br [18], ^{72,73,74,76}Kr [4,13,19–21], ^{74}Rb [13,22], and ^{76}Sr [23]. The standard parametrization of the Nilsson potential [24] was employed in the CNS calculations, whereas the NL3 parametrization was used in the CRMF calculations [25]. The results of these calculations are shown in Fig. 4, where the configurations are labeled by the number of $g_{9/2}$ protons and neutrons and the total signature as $[p, n](\alpha_{\text{tot}})$.

Figure 5 shows the experimental and calculated excitation energies minus a rigid rotor reference versus angular momentum for bands 1 through 3 and the corresponding theoretical configurations. The comparison between the theory and experiment suggests that the configurations $[4, 4](\alpha = -1/2)$, $[4, 4](\alpha = +1/2)$, and $[3, 4](\alpha = +1/2)$ should be assigned to bands 1, 2, and 3, respectively. From these configuration assignments the maximum spins

FIG. 3. (Color online) Measured and calculated best fit for values of the residual Doppler shift, $F(\tau)$ for bands (a) 2 and (b) 3 in ^{75}Rb.
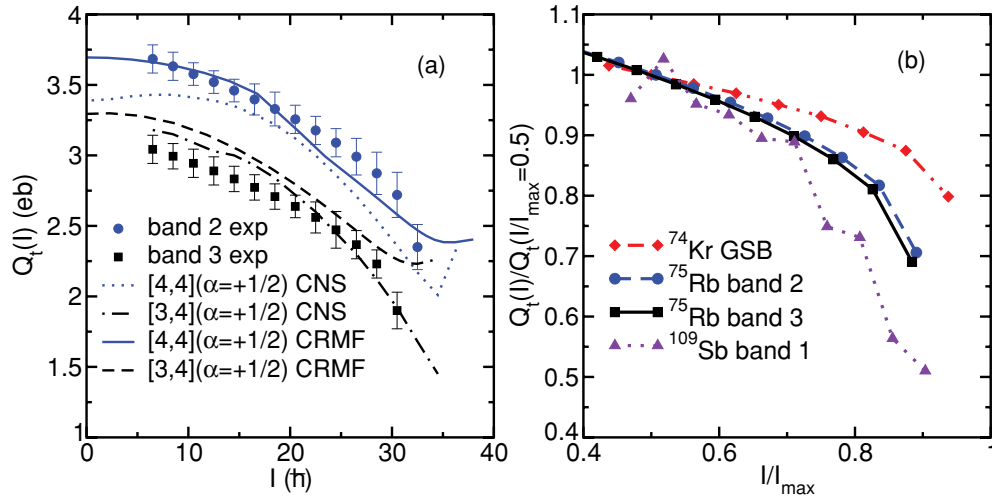
FIG. 4. (Color online) Panel (a) shows a comparison of the experimentally obtained transition quadrupole moments and those calculated using the CNS and CRMF formalisms. The $[4,4](\alpha = +\frac{1}{2})$ configuration corresponds to band 2 and the $[3,4]$ $(\alpha = +\frac{1}{2})$ configuration corresponds to band 3. Panel (b) shows the normalized transition quadrupole moments of the bands in ^{74}Kr [4], ^{75}Rb, and ^{109}Sb [26], as a function of $I/I_{\max}$. The average of transition quadrupole moments of the lowest two transitions in ^{109}Sb band 1 is used as a normalized value of $Q_t(I)/Q_t(I/I_{\max} = 0.5)$ at $I/I_{\max} = 0.5$ for this band.

$I_{\max}$, for bands 2 and 3 are calculated as $\frac{73}{2}^-$ and $\frac{69}{2}^+$, respectively. The detailed structure of the $[4,\bar{4}](\alpha = +1/2)$ configuration, with respect to the ^{56}Ni spherical core, is $\pi[g_{9/2}]_{12}^4 [f_{5/2} p_{3/2} p_{1/2}]_{6.5}^5 \otimes \nu[g_{9/2}]_{12}^4 [f_{5/2} p_{3/2} p_{1/2}]_6^6$. The superscripts and subscripts to subshell labels indicate the number of occupied orbitals within the subshell and the maximum spin built within the subshell, respectively. For example, superscript 4 and subscript 12 to $[g_{9/2}]_{12}^4$ show that four $g_{9/2}$ particles can build a maximum spin $i_{\max} = 4.5 + 3.5 + 2.5 + 1.5 = 12$. Thus, bands 2 and 3 are observed up to $I_{\max}$ and one transition short of $I_{\max}$, respectively

For the given assignments the calculations reproduce reasonably well the $(E - E_{RLD})$ curves of the observed bands 2

and 3. The relative positions of bands 1 through 3 depend on the accuracy of the description of the relative energies of different single-particle states in model calculations. The low effective mass of the CRMF approach leads to larger energy distances between calculated configurations [6]. In general, the experimental situation for bands 2 and 3 is described somewhat better in the CNS calculations.

The physics of the termination of rotational bands in nuclei with masses $A \geqslant 60$ was studied exclusively by the CNS approach [1] because of the developed technology to trace nuclear configurations over a significant spin range up to termination and the ability to provide potential energy surfaces for each configuration at each spin of interest. On the contrary,
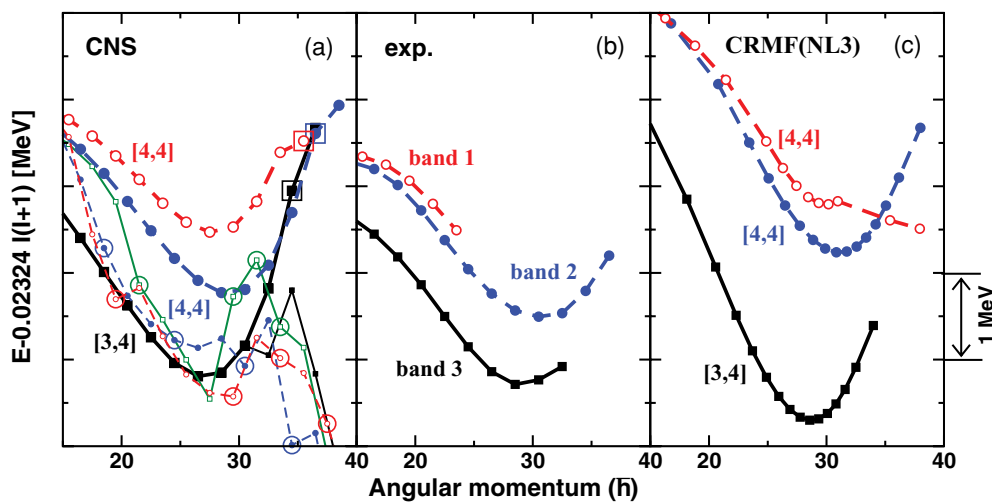
FIG. 5. (Color online) Excitation energies relative to a rigid-rotor reference E_{RLD}. Panels (a)–(c) show CNS calculations, experimental data, and CRMF calculations, respectively. Solid and dashed lines represent positive and negative parity configurations, respectively. Open and solid circles are used for signatures $\alpha = -\frac{1}{2}$ and $\alpha = +\frac{1}{2}$, respectively. Terminating (aligned) states are shown by large open circles and the states that possess some collectivity at the maximum spin $I_{\max}$ of the respective configuration by large open squares. The yrast lines for four combinations of parity and signature are shown by small symbols and thin lines in panel (a).

more microscopic calculations such as CRMF provide only information about the deformation of local minima and generally have difficulty in tracing specific configurations up to termination. The CNS calculations reveal that the rotational bands remain collective at I_{max} and that higher spin states with $I = I_{max} + 2$ can be built [Fig. 5(a)]. For example, the I_{max} state of band 3 has deformation $\varepsilon_2 = 0.22$, $\gamma = 15°$ in the CNS calculations. A clear signal of the nontermination of rotational bands can come from the observation of the $I_{max} + 2$ states in the rotational sequences. However, such states are located well above the yrast line according to the calculations [Fig. 5(a)], hence their observation is expected to be extremely difficult with the current generation of γ-ray arrays.

As follows from Ref. [4], the evolution of transition quadrupole moments as a function of spin up to or close to I_{max} also provides an important fingerprint for the nontermination of rotational bands at I_{max}. Figure 4(a) shows the experimental and calculated transition quadrupole moments as a function of spin. These values were extracted up to $\frac{65}{2}\hbar$ ($I = I_{max} - 4$) and $\frac{61}{2}\hbar$ ($I = I_{max} - 4$) for bands 2 and 3, respectively. One can see that both the evolution of the transition quadrupole moment with angular momentum and the relative transition quadrupole moments of the two bands are reasonably well described by the CNS and CRMF calculations.

Figure 4(b) shows the normalized transition quadrupole moments $Q_t(I/I_{max})/Q_t(I/I_{max} = 0.50)$ as a function of I/I_{max} for bands in ^{109}Sb [26], ^{75}Rb, and ^{74}Kr [4]. As can be seen, the transition quadrupole moments were measured to near I_{max} in all three nuclei, specifically, ^{109}Sb and ^{75}Rb are measured up to $I_{max} - 4$ and ^{74}Kr up to $I_{max} - 2$. Band 1 in ^{109}Sb, which is a classical example of smooth band termination [1,26], shows considerable drop of collectivity on approaching $I/I_{max} = 1$. On the contrary, the ground state band in ^{74}Kr, which does not terminate at I_{max} [4], shows only a marginal reduction of collectivity as I/I_{max} approaches 1. The normalized transition quadrupole moments of bands 2 and 3 in ^{75}Rb are located in between these two cases.

The nontermination of the rotational bands has its origin in the strong mixing between the low-j $p_{1/2}$, $p_{3/2}$, and $f_{5/2}$, and high-j $f_{7/2}$ orbitals in the $N = 3$ shell [3,4]. For both ^{74}Kr and ^{75}Rb mixing between low-j and high-j orbitals is a consequence of the appreciable deformation of rotational bands at low-spin and high rotational frequencies observed close to I_{max}. In the case of ^{74}Kr the smooth nature of the dynamical moments of inertia, for $\hbar\omega \equiv 0.8$ MeV, suggests that mixing between low-j and high-j orbitals takes place gradually. On the contrary, the presence of small disturbances in the dynamical moments of inertia seen at $\hbar\omega \approx 1.5$ MeV in bands 2 and 3 of ^{75}Rb (see Fig. 1) suggests that, in this case, the process is less gradual.

In conclusion, transition quadrupole moments of two rotational bands in ^{75}Rb were deduced up to two transitions short of the maximum spin I_{max}, while these bands are observed up to or one transition short of I_{max}. The normalized transition quadrupole moments as a function of I/I_{max} show behavior that is in between the classical cases of noncollective termination at I_{max} (band 1 in ^{109}Sb) and nontermination at I_{max} (bands in ^{74}Rb) of rotational bands. The CNS calculations strongly suggest that neither band will terminate at I_{max}. These results provide strong evidence for the second example of the nontermination of rotational bands at $I = I_{max}$ in any mass region. The precise measurement of transition quadrupole moments up to I_{max} and the observation of the $I_{max} + 2$ state in a rotational band will clearly be of interest to confirm this interpretation.

[1] A. V. Afanasjev, D. Fossan, G. Lane, and I. Ragnarsson, Phys. Rep. **322**, 1 (1999).
[2] T. Troudet and R. Arvieu, Ann. Phys. (NY) **134**, 1 (1981).
[3] I. Ragnarsson and A. V. Afanasjev, in *Proceedings of the Conference on Nuclear Structure at the Limits, Argonne, IL, USA, 1997* (ANL Report No. ANL/PHY-97/1, 1997), p. 184.
[4] J. J. Valiente-Dobon *et al.*, Phys. Rev. Lett. **95**, 232501 (2005).
[5] T. Steinhardt *et al.*, Phys. Rev. C **81**, 054307 (2010).
[6] A. V. Afanasjev, J. Konig, and P. Ring, Nucl. Phys. A **608**, 107 (1996).
[7] I. Y. Lee, Nucl. Phys. A **520**, 641 (1990).
[8] D. G. Sarantites *et al.*, Nucl. Instrum. Methods Phys. Res. Sect. A **381**, 418 (1996).
[9] R. A. Wyss, P. J. Davies, W. Satula, and R. Wadsworth, Phys. Rev. C **76**, 011301 (2007).
[10] C. Gross *et al.*, Phys. Rev. C **56**, R591 (1997).
[11] B. Cederwall, Nucl. Instrum. Methods Phys. Res. Sect. A **354**, 591 (1995).
[12] K. Starosta *et al.*, Nucl. Instrum. Methods Phys. Res. Sect. A **515**, 771 (2003).
[13] F. L. Johnston-Theasby *et al.*, Phys. Rev. C **78**, 034312 (2008).
[14] J. J. Valiente-Dobón *et al.*, Phys. Rev. C **71**, 034311 (2005).
[15] J. F. Ziegler, M. D. Ziegler, and J. P. Biersack, Nucl. Instrum. Methods Phys. Res. Sect. B **268**, 1818 (2010).
[16] C. J. Chiara *et al.*, Nucl. Instrum. Methods Phys. Res. Sect. A **523**, 374 (2004).
[17] C. E. Svensson *et al.*, Acta Phys. Pol. B **32**, 2413 (2001).
[18] D. Jenkins *et al.*, Phys. Rev. C **65**, 064307 (2002).
[19] N. S. Kelsall *et al.*, Phys. Rev. C **65**, 044331 (2002).
[20] A. V. Afanasjev and S. Frauendorf, Phys. Rev. C **71**, 064318 (2005).
[21] C. Andreoiu *et al.*, Phys. Rev. C **75**, 041301 (2007).
[22] C. D. O'Leary *et al.*, Phys. Rev. C **67**, 021301 (2003).
[23] P. J. Davies *et al.*, Phys. Rev. C **75**, 011302 (2007).
[24] T. Bengtsson and I. Ragnarsson, Nucl. Phys. A **436**, 14 (1985).
[25] G. A. Lalazissis, J. Konig, and P. Ring, Phys. Rev. C **55**, 540 (1997).
[26] R. Wadsworth *et al.*, Phys. Rev. Lett. **80**, 1174 (1998).